Method for arbitrary phase transformation by a slab based on transformation optics and the principle of equal optical path

Y. Ke Key Laboratory for Micro-/Nano-Optoelectronic Devices of Ministry of Education, College of Information Science and Engineering, Hunan University, Changsha 410082, China

W. Shu wxshu@hnu.edu.cn Key Laboratory for Micro-/Nano-Optoelectronic Devices of Ministry of Education, College of Information Science and Engineering, Hunan University, Changsha 410082, China

H. Luo Key Laboratory for Micro-/Nano-Optoelectronic Devices of Ministry of Education, College of Information Science and Engineering, Hunan University, Changsha 410082, China

S. Wen Key Laboratory for Micro-/Nano-Optoelectronic Devices of Ministry of Education, College of Information Science and Engineering, Hunan University, Changsha 410082, China

D. Fan Key Laboratory for Micro-/Nano-Optoelectronic Devices of Ministry of Education, College of Information Science and Engineering, Hunan University, Changsha 410082, China

The optical path lengths travelled by rays across a wavefront essentially determine the resulting phase front irrespective of the shape of a medium according to the principle of equal optical path. Thereupon we propose a method for the transformation between two arbitrary wavefronts by a slab, i.e. the profile of the spatial separation between the two wavefronts is taken to be transformed to a plane surface. Interestingly, for the mutual conversion between planar and curved wavefronts, the method reduce to an inverse transformation method in which it is the reversed shape of the desired wavefront that is converted to a planar one. As an application, three kinds of phase transformation are realized and it is found that the transformation on phase is able to realize some important properties such as phase reversal or compensation, focusing, and expanding or compressing beams, which are further confirmed by numerical simulations. The slab can be applied to realizing compact electromagnetic devices for which the values of the refractive index or the permittivity and permeability can be high or low, positive or negative, or near zero, depending on the choice of coordinate transformations.
[DOI: http://dx.doi.org/10.2971/jeos.2012.12013]

Keywords: phase transformation, wavefront, optical path length, transformation optics

1 INTRODUCTION

In the last few years, transformation optics [1, 2], based on the form-invariance of Maxwell's equations under coordinate transformations, has been attracting more and more attention. According to the equivalence of space geometry and material in routing light, it provides a robust method to control electromagnetic waves by materials usually implemented by metamaterials [3]. This has led to remarkably successful applications to designing electromagnetic devices, which may be mainly classified into four classes. The first is to control the path of light ray, such as invisibility cloaks [4]–[6], light concentrator/absorber [7, 8], beam expanders/compressors [9, 10], beam shifter [11, 12], and beam bends [13, 14]. The second is to manipulate the polarization [15] and the third is to control the amplitude [16]–[18]. While the last is to mold the phase with notable examples as the field rotators [19] and phase transformers [20]–[22].

There exists a limitation on the wave through most of the above devices yet. That is, the exit wave would return [4] or be parallel [11] to the incident wave direction, or be perpendicular to the exit interface [13] because the wave vector or phase front has not been changed by transformations. Recently, phase transformers in the last class achieved the direction of exit wave different from the incoming one, but at the cost of irregular profiles due to the direct transformation used. It is natural to ask if a device can be designed independent of the geometrical shape, such as a slab, to manipulate the exit wavefront. As well known the planar structure is preferred in practical applications, especially as plug-and-play devices, being compact enough as well as free of aberrations [23]. Indeed certain planar designs have been used to realize directive emission with high performance by transforming cylindrical waves into plane ones [24]–[29]. However a general theory for phase transformation through planar configurations has not been proposed yet.

In this work we introduce a new coordinate transformation method from the fundamental concepts of wavefront and optical path length (OPL) in ray optics to design a slab to manipulate the phase. Through the slab the conversion between two arbitrary wavefronts can be achieved. The slab can be realized by materials for which the refractive index or the permittivity and permeability can be high or low, positive or negative, or near zero, depending on the choice of transformations. The results can be applied to realizing compact electromagnetic devices, such as wave deflector, flat lens, phase compensator and

Received March 09, 2012; revised ms. received April 24, 2012; published May 18, 2012 ISSN 1990-2573

beam expander or compressor. In addition, the method takes a straightforward form and can completely avoid possible singular points in constitutional parameters.

This work is organized as follows. In Sec. 2.1 we derive from the concepts of wavefront and OPL the coordinate transformation method related to planar wavefronts, i.e. the inverse transformation method, then extend it to a general form in Sec. 2.2. In Sec. 3 we realize three kinds of phase transformation as an application of the approach and discuss the influence of the choice of coordinate transformation on material parameters. Discussion and conclusion are made in the last section.

2 THE BASIC FARMULATION

Let us begin with the concept of wavefront and OPL. As well known the wavefront is the surface of constant phase and the phase differences of any two corresponding points on two sequential wavefronts are identical [30]. The optical path lengths (OPLs) involved are also equal, stated by the principle of equal optical path [31]. In accordance with Fermat's principle, the rays across initial wavefront traverse individual paths so that the OPLs or the times of travel are extrema, whether through conventional optical components [32] or newly developed transformation media. If these OPLs are distinct, they arrive the exit surface at different moments and the associated phases are varied. Thereby the resultant wavefront is distorted according to the principle of equal optical path. So, strictly speaking, it is the OPLs travelled rather than the shape of medium that fundamentally determine the resulting phase front [31, 32]. Theoretically, therefore, one phase transformation can be realized by materials of various profiles as long as the needed OPLs, i.e. phase differences, are satisfied. On the other hand, the transformation between wavefronts corresponds to one specific coordinate transformation in a mathematical perspective [19]–[29]. Thus it is entirely feasible to construct material with a slab configuration to transform wavefront by transformation optics. These form the basis for our method.

2.1 The inverse transformation method for the transformation associated with planar wavefronts

For simplicity we consider the two-dimensional wave problem and first establish the framework of transformation to convert a planar wave front into any desired phase front. To achieve that the usual approach in literature is to transform a plane surface to the desired wave shape immediately, i.e. from $B'C'$ to $A'E'$ as shown in Figure 1(a), which may be called direct transformation method (DTM) [20]–[22]. Therein the virtual region ($OB'C'D$, enclosed by dotted lines) is transformed into the physical one ($OA'E'D$ in yellow). Such a DTM is intuitive enough but results in designs with irregular shapes, $OA'E'D$. Instead, we adopt an inverse transformation method (ITM): *the reversed shape of the desired wavefront is converted to a planar one*, i.e., from AE to BC, whereby the design is a slab, $OBCD$, as shown in Figure 1(b). Here it is the virtual region $OAED$ that is transformed into the flat physical one $OBCD$.

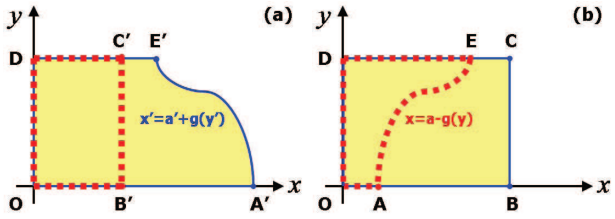

FIG. 1 Schematic diagram of the space transformation to convert a planar phase front into a curved one by (a) direct transformation method in literature and (b) inverse transformation method adopted in the present work. AE is a reversed version of $A'E'$. The dotted regions are the virtual spaces while the real-lined regions indicate the physical spaces. $OA' = a', OB' = b', OA = a, OB = b$, and $OD = d$.

In the transformation of any point from $B'C'$ to $A'E'$, the distance travelled is $g(y') + a' - b'$, where $B'C'$ is set as $x = b'$ and $A'E'$ is defined as $x' = a' + g(y')$. Instead, in the transformation way from AE corresponding to $x = a - g(y)$ into BC with $x = b$, the separation is $g(y) + b - a$. Here (x, y) is an arbitrary point in the virtual space while (x', y') in the physical space. Practically constants $a' - b'$ or $b - a$ do not affect the resulting shape of phase front, so the effective OPLs are identical between the two ways since $y = y'$. Thereupon the ITM can implement exactly the same function as DTM. In detail, the slab in Figure 1(b) can convert a planar wave front into a curved one, the opposite shape of AE, which is just the function of $OA'E'D$ in Figure 1(a). Meanwhile, within the context of DTM the slab should be capable of converting a curved wave AE into a plane wave BC. Therefore the slab by ITM has a twofold function which we denote by I and II, respectively. For simplicity, we do not consider the transformation in the y direction.

By ITM the spatial distortion can be recorded as a mapping between the original and transformed spaces,

$$x' = \rho(x,y)\frac{bx}{\Delta}, \quad y' = y, \quad z' = z, \tag{1}$$

where $\rho(x, y)$ is a scaling factor and

$$\Delta = a - g(y) \tag{2}$$

corresponding to AE, the reversed shape of the wanted wavefront. The mapping means that the virtual space is stretched or squeezed proportionally into the physical space. Theoretically one can choose a transform freely [1, 2]. The present choice is made as $\rho(x, y) = 1$ in order that the parameters change linearly and the slab can be implemented easily. The difference from the literature is that it has such a simplicity that it needs not consider the details of transformation. According to transformation optics, the permittivity tensor $\boldsymbol{\varepsilon}$ and permeability tensor $\boldsymbol{\mu}$ in the transformed coordinate system are connected with the original $\boldsymbol{\varepsilon_o}$ and $\boldsymbol{\mu_o}$ by the relationships: $\boldsymbol{\varepsilon} = J\boldsymbol{\varepsilon_o}J^T/\det(J)$, $\boldsymbol{\mu} = J\boldsymbol{\mu_o}J^T/\det(J)$ where $J_i^{i'} = \partial x^{i'}/\partial x^i$ is the Jacobian transformation matrix [3]. Applying Eq. (1) gives a general result of the relative material parameters for the conversion between plane wave and arbitrarily curved wavefront:

$$\boldsymbol{\varepsilon} = \boldsymbol{\mu} = \begin{bmatrix} \frac{b}{\Delta} + \frac{x^2\Delta'^2}{b\Delta} & -\frac{x\Delta'}{b} & 0 \\ -\frac{x\Delta'}{b} & \frac{\Delta}{b} & 0 \\ 0 & 0 & \frac{\Delta}{b} \end{bmatrix}, \tag{3}$$

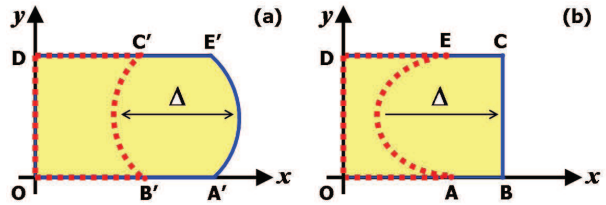

FIG. 2 Schematic diagram of the space transformation to convert a curved phase front into another curved one by (a) direct transformation method in literature and (b) the transformation method in the present work. AE, a profile of the spatial separation of the two wavefronts $B'C'$ and $A'E'$, is taken to be transformed into a plane.

where $\Delta' = \partial\Delta/\partial y$ and the original space is considered as vacuum. Notice that the superscripts of coordinate variables have been omitted for simplicity. No singularity exists for $\boldsymbol{\varepsilon}$ and $\boldsymbol{\mu}$ as long as AE does not intersect with y-axis. Thereupon, the problem of singularity [27, 28] arising mathematically can be avoided completely by taking appropriate transformation ways. It is important to note that the complex amplitude transmittance [33] of electromagnetic wave through the slab can be written as

$$t = e^{-ik_0\Delta}, \tag{4}$$

where k_0 is the free-space wavenumber and the constant phase factor has been omitted.

2.2 The general transformation method for the transformation between two arbitrary wavefronts

In an analogous fashion to the above discussion, we now examine how to convert a curved wave front into any desired one by a slab. Figure 2 applies as a sketch wherein $B'C'$ is curved now. The DTM in literature is to transform a curved wave to the desired wave shape immediately, i.e. from $B'C'$ to $A'E'$, and results in designs with irregular shapes, $OA'E'D$. Here, we generalize the ITM following the same principle based on OPL. Briefly, one also can imagine compressing $A'E'$ into a plane BC, then the original $B'C'$ would undergo the same distortion in the x direction becoming AE. However, the transformation becomes that *the profile of the spatial separation between the original and desired wavefronts is converted to a plane surface*, i.e. from AE to BC, to realize the design by a slab as $OBCD$ in Figure 2(b).

In transforming any point from $B'C'$ to $A'E'$, the distance experienced is $g_2(y) - g_1(y') + a' - b'$, where $B'C'$ and $A'E'$ are supposed to be $x' = b' + g_1(y')$ and $x = a' + g_2(y)$, respectively. Instead, in the transformation way from AE with $x = a + g_1(y) - g_2(y)$ to BC with $x = b$, the separation traversed is $g_1(y) - g_2(y) + b - a$. Actually $a' - b'$ or $b - a$ do not affect the resulting shape of front, so the effective OPLs are identical for the two ways since $y = y'$. Therefore the results Eqs. (1) and (3) still hold true except that Δ now becomes

$$\Delta = a + g_1(y) - g_2(y) \tag{5}$$

corresponding to the profile of spatial separation between the two wavefronts. If the incident wavefront is planar, e.g. $a + g_1(y) = b'$, then $\Delta = b' - g_2(y)$, which is the reversed shape of the outgoing wavefront. That is to say, to transform a plane wave into a curved wavefront by a slab, it only needs to transform the reversed shape of the latter into the former. This is just the above conclusion of Eq. (2), so Eq. (5) is a general result.

It is important to note that in deriving Eq. (2) or Eq. (5), AE should be shifted so as not to intersect the y axis to avoid the singularity in $\boldsymbol{\varepsilon}$ and $\boldsymbol{\mu}$ in Eq. (3). That is, Δ can be added with a constant that will not change the generated wavefront, but only affect the values of $\boldsymbol{\varepsilon}$ and $\boldsymbol{\mu}$ in the slab. We will address this point later.

3 APPLICATION OF THE TRANSFORMATION METHOD

Applying the above method, a wavefront can be converted into any desired one through a slab with $\boldsymbol{\varepsilon}$ and $\boldsymbol{\mu}$ determined by Eq. (3). In the following we discuss three kinds of phase transformation to illustrate the method. Incidentally, similar wavefronts could have been generated by other media using different methods somewhere in literature, e.g. conventional lens or transformation media, but our principal emphasis is on the new general method used to design *flat* media to induce phase shift and bend wavefront.

3.1 Planar to planar wavefront transformation.

Suppose a plane wave to be deflected into other directions by the slab. Without loss of generality, the reversed wavefront AE is chosen as $y = -(x - a)\cot\theta$ such that the exit wave is deflected clockwise by an amount θ. Then

$$\Delta = a - y\tan\theta \tag{6}$$

and using Eq. (3) one obtains the relative material parameters for the slab.

To test the effectiveness of the ITM and the proposed design, suppose $a = 0.4$m, $b = 0.3$m and $\theta = \pi/6$. Consider a z-polarized Gaussian beam with a wavelength of $\lambda = 0.05$m incident on the slab of $d = 0.8$m (the choices are uniform throughout), the electric field distribution obtained from a finite-element simulation is shown in Figure 3. We see that the incident wavefront is gradually tilted inside the slab until the deflection result is transferred out to the free space. The exit beam acquires a new direction of propagation unlike that of the incident one and the deflected wavefront is not necessarily parallel to the exit interface. Interestingly, by comparing (a) and (b) we find that the beam is deflected by the same amount whether for normal or oblique incidence. The underlying mechanism is that this transformation is in fact an operation of rotation on the local coordinate system which will be imposed on any fixed incident field vectors, resulting in wave vectors with identical deflection. This fact confirms the twofold function of the slab: *I*-Convert a normally incident plane wave into another with the deflected angle θ; *II*-Convert an oblique plane wave with the incident angle $-\theta$ into a normal one. Also the ITM is justified.

To change the deflection amount, one can adjust the parameter

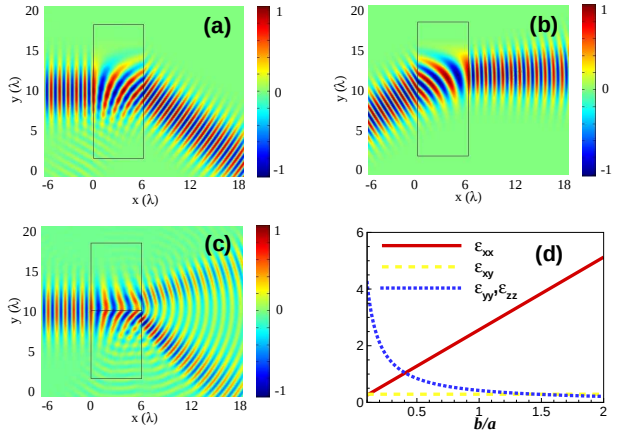

FIG. 3 Normalized E-field patterns in the slab deflector for (a) normal incidence with exit angle $\pi/6$ and (b) incident angle $-\pi/6$ with normal outgoing, and (c) in a splitter formed by the upper slab with deflection angle of $-\pi/12$ and the lower of $\pi/6$. (d) The permittivity at the center of the slab varies with the width b.

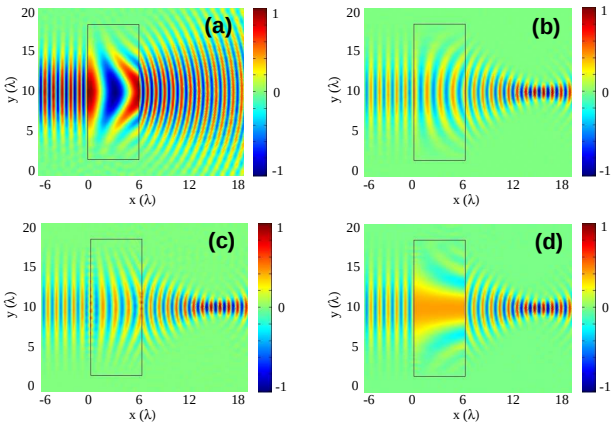

FIG. 4 Normalized E-field patterns in the slab applying (a) *converging*/(b,c,d) *diverging* surface to planar one transformation. The slab can convert a planar wavefront to a (a) *diverging*/(b,c,d) *converging* one. The surfaces to transform are chosen as $\Delta = 0.05 + (y-0.5)^2$ in (a), $0.2-(y-0.5)^2$ in (b), $-0.2-(y-0.5)^2$ in (c), and $-(y-0.5)^2$ in (d). The incident beam centers are $(0, 0.5)$ and the waists w_0 are 0.2m.

θ. Positive or negative θ, i.e. clockwise or counter-clockwise deflection, even extreme angles approaching the boundary, can be realized. Alternatively, one can realize different deflections by stacking certain pieces of slabs with given deflection amounts. In addition, combine two such slabs and a beam splitter is created, e.g. Figure 3(c). A benefit of this splitter is that a beam can be split into any two directions, provided that the deflection angles are set accordingly. We also find that the width b can be chosen freely, so the slab can be made as compact as desired only at the expense of a larger range of material parameters, as shown in Figure 3(d).

3.2 Planar to curved wavefront transformation.

For example, we consider how to convert a plane wave to a diverging/converging wave. AE is assumed to be a paraboloid

$$\Delta = a - y^2/2R(a) \tag{7}$$

positioned at $x = a$ where the radius of curvature

$$R(x) = \pm x(1 + x_0{}^2/x^2) \tag{8}$$

and the Rayleigh range $x_0 = w_0^2\pi/\lambda$ corresponding to a Gaussian beam of waist radius w_0. Eqs. (7) and (8) will be of continuous use from now on. Applying the ITM, the inverse transformation is taken from a converging/diverging surface to a planar one. Then the material parameters are obtained by using Eq. (3). Similar transformations were used to generate plane waves [25, 26], but here we make use of the map inversely.

In order to show the phase evolution clearly, we choose $a = 0.05\text{m}/0.2\text{m}$. The other values are $w_0 = 0.2\text{m}$, $R = -0.5\text{m}/0.5\text{m}$ and the waist center $(0, 0.5)$ for the incident beam which approximates a planar wavefront, and the simulated results are shown in Figure 4(a)/(b). Note that we have adopted the convention that a converging wavefront has a negative radius of curvature whereas a diverging wavefront has a positive radius of curvature. In the slab one can see the incident planar wavefront gradually evolves into a diverging/converging one at $x = b$, i.e., the function I. The central area of the wavefront travels faster/more slowly than its outer edges and then the midregion overtakes/lags behind those edges, thereby continuously bending the wavefront. In terms of Fermat's principle, it means that the refractive index is lower/larger in the central than in outer edges. In Figure 1 the generated surface $A'E'$ is the mirror image of the transformed surface AE, so one can see that the radius of exit phase surface is $0.5\text{m}/-0.5\text{m}$ just contrary to R and the new waist varies accordingly.

On the other hand, the slab in (a)/(b) enables *II*-make a converging/diverging wavefront bend into a planar one, as shown in the literature applying similar coordinate transformations [24]–[27]. Hence the slab also has a twofold function which may find import applications. For instance, it is capable of implementing flat lens. Recall that for a thin lens the complex amplitude transmittance is $t = e^{ik_0nb_0 - ik_0y^2/2f}$, where n is the refractive index, b_0 is the thickness of the center, and f is the focal length [33]. Therefore, the slab determined by Eq. (7) is equivalent to a thin lens with the focal length $f = R$, which was confirmed by Figure 4. Apart from its shape being a compact slab, such a lens has another advantage that the location of focus can be tuned continuously by changing the material parameters or discretely by stacking certain pieces of slab with unit focus distances. Note that the result in (b) is very similar to but nevertheless distinct from previous results of flattening lens [34, 35]. The transformation in the latter was to reshape a known optical component, whereas the present method immediately take the wavefront to transform and thus is endowed with great flexibility, so results $\boldsymbol{\varepsilon}$ and $\boldsymbol{\mu}$ are different, too.

To examine the role the factor a plays in the result, we alter its value in (b) as $a = -0.2\text{m}$ and 0m, and the results are shown in (c) and (d), respectively. Note that the original wavefront in (c) and (d) are chosen left to the slab, whereas that in (b) is inside the slab. Comparing (b) and (c) or (d), one can readily see that the period number of wave inside the slab equals a/λ. This fact can be understood by Figure 1 where the original wave distribution in $OAED$ is transformed into that in $OBCD$

and $OA = a$, so the period number of the original wave along OA is just that in the slab along OB. Particularly interesting is the crest in (d) that becomes quite elongated and stretches into a long beam inside the slab, exhibiting a extremely large wavelength. Correspondingly, the index of refraction should be nearly zero [36], which will be proved later.

At the same time, it can be seen from (b), (c) and (d) that the exit wavefronts remain fixed, converging at a point R away from the slab. This fact results from that the curvature of radius in the transform is uniform. So they can implement the same function and thus the original surface AE in Figure 1 need not be chosen in the slab. Particularly, in contrast with (b), it seems like that the central region of wavefront travelled faster than the outer edges inside the slab in (c) and (d), like in (a). However, the fact is quite the contrary and the true reason is that negative refraction occurs in (c) and (d), thereby introducing negative phase shift. Since the central area of the beam travels more slowly than its outer edges, the subtracted phase is less and the accumulated phase of the midregion is advanced with respect to those edges on the back surface, whereby the outgoing wavefront are deformed as in (b). This point is evident from the opposite phases traversing the boundary in (c) and (d). Such a process leads to the *reversal of phase* that may find important applications, such as wavefront correction in imaging or adaptive optics. In contrast the phases across the interfaces are uniform in (a)/(b) and the refractive indexes are positive. Therefore, we come to an important conclusion that the ways to get a desired wave are diverse and then the same to the choices of slab, thereby increasing the possibility of realization.

3.3 Curved to curved wavefront transformation.

To be specific we investigate the conversion of a diverging wave $x = a + g_1(y)$ with $a = 0.3$m, $R = 0.5$m and the beam center $(-0.15, 0.5)$ to a converging one $g_2(y)$ with $R' = -1.2$m, where Eqs. (7) and (8) have been applied. Then the material parameters are obtained by using Eqs. (3) and (5), and the simulated results are shown in Figures 5(a) and 5(b). Apparently the left diverging wave traversing the slab is deformed into a converging one. As in the above subsection, the period number of wave inside the slab equals a/λ and R' determines the generated wavefront radius of curvature. At the same time, the slab induces a transmittance the same as that of a thin lens with the focal length satisfying $1/f = 1/R - 1/R'$. Moreover, the focus can be tuned continuously by changing the parameters of transformation. For example, let $-a$ equals to the distance of beam center from the slab, then the beam will focus at the exit surface, as shown in Figure 5(c). The reason is that the choice of transformation is to let the wavefront at $-a$, i.e. incident beam center, be converted to a plane surface. The slab now acts as a *phase compensator* that reverses the amount of phase change within the region a away from the slab. Therefore, it is expectable that, if $-a$ is larger than the distance of beam center from the slab, then the beam will *focus* inside the slab, as shown in Figure 5(d). Such a function can be utilized as beam relaying and flat lens [23, 34, 35].

As known beam expansion or compression has been achieved

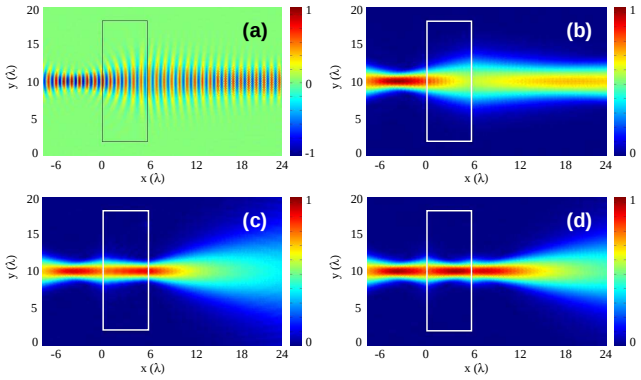

FIG. 5 Normalized E-field patterns (a) and the energy density (b,c,d) in the slab transforming a diverging wavefront to a converging one. (c) displays the focus on the exit boundary when $-a$ equals to the distance of beam center from the slab. If $-a$ becomes larger, then another focus will appear inside the slab, leading to focusing of light in (d). The two wavefronts are chosen as (a,b) $a + g_1(y) = 0.3 - (y - 0.5)^2$, (c) $a + g_1(y) = -0.15 + (y - 0.5)^2$, (d) $a + g_1(y) = -0.3 + (y - 0.5)^2$, while $g_2(y) = (y - 0.5)^2/2.4$ and incident beam center $(-0.15, 0.5)$.

by manipulating the longitudinal energy flow [9, 13], that is, expanding or squeezing the virtual space in the y direction in Figure 1. In contrast, the same task can be performed now by the transformation on the transverse phase, that is, distorting the virtual space in the x direction. From the above, the wavefront with the radius of curvature R at a is transformed into another one with the radius of curvature R' at b. The widths of the two waves, w and w' across the back interface can be considered unchanged. Then, for the outgoing wave, in accordance with R' and w', the beam center x away from the slab and the waist radius w_0' can be found, i.e., $x = -R'/[1 + (\lambda R'/\pi w'^2)^2]$ and $w_0' = w'^2/[1 + (\pi w'^2/\lambda R')^2]$. Therefore, the width of the resultant beam can be engineered through choosing appropriate wavefront to transform and R'. In Figures 5(a) and 5(b), the wavefront transformed with a distance from the center $x = 0.45$m has a width $w = w_0\sqrt{1 + (x/x_0)^2} = 0.15$m, so the waist radius of the resulted beam equals to $w_0' = 0.1$m, two times the original one. Evidently, the incident beam is expanded into another one with wider waist. The contrary condition, beam compression, can be realized similarly.

3.4 Influence of the coordinate transform on material parameters.

Next we discuss the effect of the choice of transformation on the material parameters. As the above analysis indicates, e.g. Figure 3(d), the values of $\boldsymbol{\varepsilon}$ and $\boldsymbol{\mu}$ change as the slab thickness varies. On the other hand, the sign and magnitude of Δ also plays an important role in determining $\boldsymbol{\varepsilon}$ and $\boldsymbol{\mu}$. We have known from Section 2 that to avoid the singularity in $\boldsymbol{\varepsilon}$ or $\boldsymbol{\mu}$, AE, i.e. Δ, can be shifted some amount along the x axis. Despite no impact on the generated wavefront, it undoubtedly influences the values of $\boldsymbol{\varepsilon}$ and $\boldsymbol{\mu}$ in the slab. From Eq. (3) we conclude that: (i) The larger the magnitude of Δ, the larger the range of values of $\boldsymbol{\varepsilon}$ and $\boldsymbol{\mu}$. In terms of the principle of the equality of OPL, wave need to travel longer path Δ to generate the phase difference and then a width-fixed slab has to increase the magnitudes of $\boldsymbol{\varepsilon}$ and $\boldsymbol{\mu}$. (ii) If Δ becomes negative, $\boldsymbol{\varepsilon}$ and $\boldsymbol{\mu}$ will also take negative values. Especially, if Δ becomes

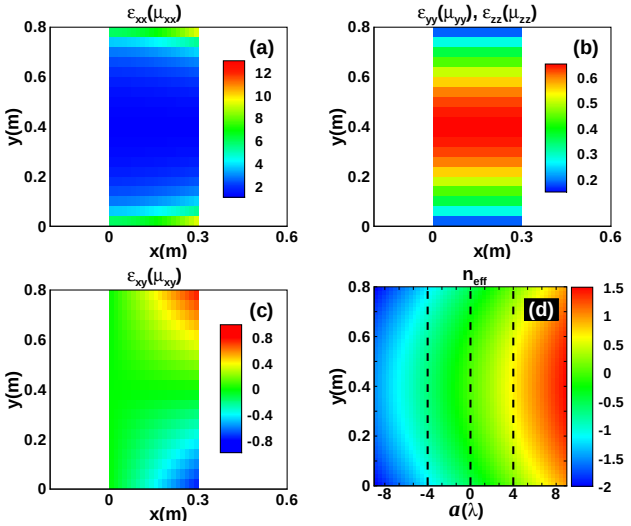

FIG. 6 (a), (b) and (c) respectively corresponds to $\varepsilon_{xx}(\mu_{xx})$, $\varepsilon_{yy}(\mu_{yy})/\varepsilon_{zz}(\mu_{zz})$ and $\varepsilon_{xy}(\mu_{xy})$. (d) shows the effective refractive index on the transverse of the slab for different choices of a with $b = 0.3$. The three dashed lines in (d) from left to right correspond to n_{eff} for slabs in Figures 4 (c), (d), (b) respectively.

zero, $\boldsymbol{\varepsilon}$ and $\boldsymbol{\mu}$ would approach infinity. In this case, Δ can be added a positive constant. As an example, we present the constitutional parameters in Figures 6(a)–(c) corresponding to the slab in Figures 4(b).

Further, in order to characterize the slab more clearly and commonly we introduce the effective average refractive index [32, 33, 37, 38] in terms of the complex amplitude transmittance Eq. (4),

$$n_{eff} = \frac{\Delta}{b}. \tag{9}$$

It indicates that the anisotropy is reduced such that nondiagonal elements in J are eliminated by choosing orthogonal grids in virtual space to transform. Then the slab can be considered as nonmagnetic and be realized by dielectrics only though the performance may be sacrificed a bit [37, 38]. The effective refractive index on the transverse of the slab for different choices of a are shown in Figure 6(d) which has included the results in Figures 4(b)–(d). It shows that n_{eff} increases with a and that n_{eff} in the center region is larger than in the outer area. This is reasonable because the larger a, the more original space will be squeezed into the slab in Figure 1(b). For the midregion, if $a \leq 0$, then $n_{eff} \leq 0$, e.g., the left two lines in Figure 6(d) corresponding to n_{eff} for slabs in Figures 4(d) and 4(c), respectively. Accordingly, the choice of transformations determines whether the values of n_{eff} or $\boldsymbol{\varepsilon}$ and $\boldsymbol{\mu}$ are high or low, positive or negative, or near zero. Therefore, it needs to take all factors into consideration and select appropriate values to realize the design by materials available.

4 DISCUSSION AND CONCLUSION

Before concluding this work it merits some further discussions. First, to implement the above design, metamaterial is competent without any technological difficulties [39, 40]. Now another simpler way is to further discretize the material parameters and build by dielectrics, which has been proved efficient to realize lossless and broadband transformation devices [23, 34, 35, 37, 41, 42]. Second, according to the principle of equal optical path the method can be generalized to realize arbitrary phase conversion through media with arbitrary geometric shapes. The coordinate transformation should guarantee that the needed OPLs are satisfied. Last, we only considered the transformation in two dimensions. Actually, the method is applicable to three-dimensional problems and more new phenomena may be found. For example, the method can be used to transform planar wavefront of Gaussian beam into helical one of vortex beam carrying orbital angular momentum [43].

In summary, we have proposed a planar phase transformer to achieve the conversion between any two wavefronts. From the point of view of OPL we present a general method of transformation wherein the profile determined by the difference of the two wavefronts is taken to be converted to a plane surface. For the mutual conversion between planar and curved wavefronts, the method is greatly simplified as the ITM in which it is the opposite shape of the desired wavefront that is converted to a plane. Applying the method, three types of phase transformation are investigated, which can be used for wave deflector and flat lens, and are further confirmed by numerical simulations. In addition, we find that the transformation on phase can realize some important properties such as phase reversal or compensation, focusing, and expanding or compressing beams. The slab can be realized by materials whose values of refractive index or $\boldsymbol{\varepsilon}$ and $\boldsymbol{\mu}$ depend on the choice of transformations. The method provides a new insight into transformation optics and we expect it will be of practical importance for designing compact optical devices.

5 ACKNOWLEDGEMENTS

This work was supported in part by the National Natural Science Foundation of China (No.10847121, 10804029, 10904036, 61025024) and the Growth Program for Young Teachers of Hunan University.

References

[1] J. B. Pendry, D. Schurig, and D. R. Smith, "Controlling electromagnetic fields," Science **312**, 1780–1782 (2006).

[2] U. Leonhardt, "Optical conformal mapping," Science **312**, 1777–1780 (2006).

[3] D. Schurig, J. B. Pendry, and D. R. Smith, "Calculation of material properties and ray tracing in transformation media," Opt. Express **14**, 9794–9804 (2006).

[4] D. Schurig, J. J. Mock, B. J. Justice, S. A. Cummer, J. B. Pendry, A. F. Starr, and D. R. Smith, "Metamaterial electromagnetic cloak at microwave frequencies," Science **314**, 977–980 (2006).

[5] B. L. Zhang, Y. Luo, X. G. Liu, and G. Barbastathis, "Macroscopic invisibility cloak for visible light," Phys. Rev. Lett. **106**, 033901 (2011).

[6] X. Z Chen, Y. Luo, J. J. Zhang, K. Jiang, J. B. Pendry, and S. Zhang, "Macroscopic invisibility cloaking of visible light," Nat. Commun. **2**, 176 (2011).

[7] M. Rahm, D. Schurig, D. A. Roberts, S. A. Cummer, D. R. Smith, and J. B. Pendry, "Design of electromagnetic cloaks and concentrators using form-invariant coordinate transformations of Maxwell's equations," Photonics Nanostruct: Fundam. Appl. **6**, 87–95 (2008).

[8] E. E. Narimanova and A. V. Kildishev, "Optical black hole: broadband omnidirectional light absorber," Appl. Phys. Lett. **95**, 041106 (2009).

[9] X. F. Xu, Y. J. Feng and T. Jiang, "Electromagnetic beam modulation through transformation optical structures," New J. Phys. **10**, 115027 (2008).

[10] C. García-Meca, M. M. Tung, J. V. Galán, R. Ortuño, F. J. Rodríguez-Fortuño, J. Martí and A. Martínez, "Squeezing and expanding light without reflections via transformation optics," Opt. Express **19**, 3562–3575 (2011).

[11] M. Rahm, S. A. Cummer, D. Schurig, J. B. Pendry, and D. R. Smith, "Optical design of reflectionless complex media by finite embedded coordinate transformations," Phys. Rev. Lett. **100**, 063903 (2008).

[12] I. Gallina, G. Castaldi, V. Galdi, A. Alù, and N. Engheta, "General class of metamaterial transformation slabs," Phys. Rev. B **81**, 125124 (2010).

[13] M. Rahm, D. A. Roberts, J. B. Pendry, and D. R. Smith, "Transformation-optical design of adaptive beam bends and beam expanders," Opt. Express **16**, 11555–11567 (2008).

[14] Y. Liu, T. Zentgraf, G. Bartal, and X. Zhang, "Transformational plasmon optics," Nano Lett. **10**, 1991–1997 (2010).

[15] D. H. Kwon and D. H. Werner, "Polarization splitter and polarization rotator designs based on transformation optics," Opt. Express **16**, 18731–18738 (2008).

[16] Y. Luo, J. Zhang, L. Ran, H. Chen and J. A. Kong, "Controlling the emission of electromagnetic source," PIERS **4**, 795–800 (2008).

[17] N. Kundtz, D. A. Roberts, J. Allen, S. Cummer, and D. R. Smith, "Optical source transformations," Opt. Express **16**, 21215–21222 (2008).

[18] J. Li, S. Han, S Zhang, G. Bartal, and X. Zhang, "Designing the Fourier space with transformation optics," Opt. Lett. 34, 3128–3120 (2009).

[19] H. Y. Chen, B. Hou, S. Y. Chen, X. Y. Ao, W. J. Wen, and C. T. Chan, "Design and experimental realization of a broadband transformation media field rotator at microwave frequencies," Phys. Rev. Lett. **102**, 183903 (2009).

[20] W. X. Jiang, T. J. Cui, H. F. Ma, X. Y. Zhou, and Q. Cheng, "Cylindrical-to-plane-wave conversion via embedded optical transformation," Appl. Phys. Lett. **92**, 261903 (2008).

[21] G. X. Yu, W. X. Jiang and T. J. Cui, "Beam deflection and splitting using transformation optics," Cent. Eur. J. Phys. **9**, 183–188 (2011).

[22] H. Ma, S. B. Qu, Z. Xu, and J. F. Wang, "General method for designing wave shape transformers," Opt. Express **16**, 22072–22082 (2008).

[23] N. Kundtz and D. R. Smith, "Extreme-angle broadband metamaterial lens," Nat. Mater. **9**, 129–132 (2010).

[24] J. J. Zhang, Y. Luo, S. Xi, H. S. Chen, L. X. Ran, B. I. Wu, and J. A. Kong, "Directive emission obtained by coordinate transformation," PIERS **81**, 437–446 (2008).

[25] D.-H. Kwon and D. H. Werner, "Transformation optical designs for wave collimators, flat lenses and right-angle bends," New J. Phys. **10**, 115023 (2008).

[26] L. Lin, W. Wang, J. Cui, C. L Du, and X. G. Luo, "Design of electromagnetic refractor and phase transformer using coordinate transformation," Opt. Express **16**, 6815–6821 (2008).

[27] P.-H. Tichit, S. N. Burokur, D. Germain, and A. de Lustrac, "Design and experimental demonstration of a high-directive emission with transformation optics," Phys. Rev. B **83**, 155108 (2011).

[28] F. Kong, B. Wu, J. A. Kong, J. Huangfu, and S. Xi, "Planar focusing antenna design by using coordinate transformation technology," Appl. Phys. Lett. **91**, 253509 (2007).

[29] Y. Luo, L. X. He, S. Z. Zhu, H. L. W. Chan, and Y. Wang, "Flattening of conic reflectors via a transformation method," Phys. Rev. A **84**, 023843 (2011).

[30] E. Hecht, *Optics* (Addison-Wesley, San Francisco, 2002).

[31] M. Born and E. Wolf, *Principles of Optics* (Cambridge University Press, Cambridge, 1999).

[32] B. E. A. Saleh and M. C. Teich, *Fundamentals of Photonics* (John Wiley & Sons, New Jersey, 2007).

[33] J. W. Goodman, *Introduction to Fourier Optics* (McGraw-Hill Companies, San Francisco, 1996).

[34] D. A. Roberts, N. Kundtz, and D. R. Smith, "Optical lens compression via transformation optics," Opt. Express **17**, 16535–16542 (2009).

[35] R. Yang, W. X. Tang, Y. Hao, and I. Youngs, "A coordiante transformation based broadband flat lens via microstrip array," IEEE Antenn. Wirel. Pr. **10**, 99–102 (2011).

[36] R. W. Ziolkowski, "Propagation in and scattering from a matched metamaterial having a zero index of refraction," Phys. Rev. E **70**, 046608 (2004).

[37] J. Li, and J. B. Pendry, "Hiding under the carpet: a new strategy for cloaking," Phys. Rev. Lett. **101**, 203901 (2008).

[38] W. X. Tang, C. Argyropoulos, E. Kallos, W. Song, and Y. Hao, "Discrete coordinate transformation for designing all-dielectric flat antennas," IEEE Trans. Antennas Propag. **58**, 3795–3804 (2010).

[39] T. J. Cui, D. R. Smith, and R. P. Liu, *Metamaterials* (Springer, New York, 2010).

[40] Z. H. Jiang, M. D. Gregory, and D. H. Werner, "Experimental demonstration of a broadband transformation optics lens for highly directive multibeam emission," Phys. Rev. B **84**, 165111 (2011).

[41] T. C. Han and C.-W. Qiu, "Isotropic nonmagnetic flat cloaks degenerated from homogeneous anisotropic trapeziform cloaks," Opt. Express **18**, 13038–13043 (2010).

[42] M. Gharghi, C. Gladden, T. Zentgraf, Y. Liu, X. Yin, J. Valentine, and X. Zhang, "A Carpet Cloak for Visible Light," Nano Lett. **11**, 2825–2828 (2011).

[43] A. M. Yao and M. J. Padgett, "Orbital angular momentum: origins, behavior and applications," Adv. Opt. Photon. **3**, 161–204 (2011).